

AD-A257 206

TION PAGE

Form Approved
OMB No. 0704-0188Pu
ga
co
Davis Highway, Suite 100, Springfield, MA 01104

Page 1 hour per response, including the time for reviewing instructions, searching existing data sources, gathering the collection of information. Send comments regarding this burden estimate or any other aspect of this Washington Headquarters Services, Directorate for Information Operations and Reports, 1215 Jefferson Management and Budget, Paperwork Reduction Project (0704-0188) Washington, DC 20503

1. AGENCY USE ONLY (Leave blank)		2. REPORT DATE		3. REPORT TYPE AND DATES COVERED Reprint	
4. TITLE AND SUBTITLE Title shown on Reprint				5. FUNDING NUMBERS DAA03-89-K-0058	
6. AUTHOR(S) Authors listed on Reprint					
7. PERFORMING ORGANIZATION NAME(S) AND ADDRESS(ES) Univ. of Minnesota Minneapolis, Minn. 55455				8. PERFORMING ORGANIZATION REPORT NUMBER	
9. SPONSORING / MONITORING AGENCY NAME(S) AND ADDRESS(ES) U. S. Army Research Office P. O. Box 12211 Research Triangle Park, NC 27709-2211				10. SPONSORING / MONITORING AGENCY REPORT NUMBER ARO 26296.3-CH	
11. SUPPLEMENTARY NOTES The view, opinions and/or findings contained in this report are those of the author(s) and should not be construed as an official Department of the Army position, policy, or decision, unless so designated by other documentation.					
12a. DISTRIBUTION / AVAILABILITY STATEMENT Approved for public release; distribution unlimited.				12b. DISTRIBUTION CODE	
13. ABSTRACT (Maximum 200 words) ABSTRACT SHOWN ON REPRINT 92-28023 1068 OCT 27 1992					
14. SUBJECT TERMS				15. NUMBER OF PAGES	
				16. PRICE CODE	
17. SECURITY CLASSIFICATION OF REPORT UNCLASSIFIED		18. SECURITY CLASSIFICATION OF THIS PAGE UNCLASSIFIED		19. SECURITY CLASSIFICATION OF ABSTRACT UNCLASSIFIED	
				20. LIMITATION OF ABSTRACT UL	

AGGREGATION BEHAVIOR OF MIXED-COUNTERION DOUBLE-CHAINED
SURFACTANTS

D. D. Miller

Eastman Kodak Company
Research Laboratories
Rochester, NY 14650-2110

and

D. F. Evans

Department of Chemical Engineering
and Materials Science
University of Minnesota
Minneapolis, MN 55455

The aggregation behavior of dilute solutions of the ditetradecyldimethylammonium surfactant cation with mixtures of bromide and acetate counterions was studied using video enhanced microscopy, cryo-transmission electron microscopy, and time resolved fluorescence quenching. Large liposomal aggregates of the bromide surfactant are gradually transformed into micellar aggregates by the addition of the acetate surfactant. Stable, equilibrium, unilamellar vesicles predominate at intermediate concentrations (40-60% Br⁻), while small, spherical micelles coexist with, and gradually replace, vesicles as the bromide content is further reduced. Similar behavior is seen with long chain-short chain phospholipid mixtures. These results are analyzed in terms of free energy minimization and bilayer asymmetry arguments.

INTRODUCTION

Recent theoretical^{1,2} and experimental^{3,4} work has demonstrated the role of mixed surfactants in stabilizing certain surfactant microstructures. Carnie et al.¹ and Safran et al.² have quantitatively proved that equilibrium, single-walled vesicles are stabilized by having different surfactant compositions in the inner and outer leaves of the bilayer. On an intuitive level the necessity of such asymmetry seems reasonable; the inner and outer layers of a vesicle have different curvatures and impose different packing constraints on the surfactant.

As pointed out by Safran, most experimental evidence for spontaneous, single-walled vesicles has indeed come from systems in which two or more surfactants were employed. Recent examples include the single chained cationic-anionic mixtures of Kaler et al.³ and the long chain-short chain phospholipid mixtures of Gabriel and Roberts.⁴

In this paper, we explore a third route to forming spontaneous vesicles. By employing mixtures of bromide and acetate counterions in dialkyldimethylammonium surfactants, a variety of microstructures are formed as the counterion composition changes. Using video enhanced microscopy, cryo-TEM, and fluorescence quenching techniques, we conclude that spontaneous vesicles dominate at intermediate compositions (40-60% Br⁻), while small, spherical micelles coexist with, and gradually replace, vesicles as the bromide level is further decreased.

EXPERIMENTAL

Materials

The preparation of dialkyldimethylammonium bromides and acetates (2C_xN⁺2C_lBr⁻ or -OAc⁻) has been described elsewhere.^{5,6} All phospholipids were purchased from Avanti Polar Lipids (Birmingham, AL) and used as received. Pyrene (Eastman Kodak) was recrystallized twice from 200-proof alcohol. Dibutylaniline (DBA, Eastman Kodak) was used as received.

Video Enhanced Microscopy (VEM)

Video enhanced differential interference contrast microscopy allows direct visualization of colloidal particles as small as 50nm. Detailed descriptions and discussions of the technique have appeared elsewhere.^{7,8} Real time background subtraction and image enhancement were performed with a Psicom 327 digital image processor (Perceptive Systems, Houston, TX).

Cryo-Transmission Electron Microscopy (Cryo-TEM)

High resolution, direct images of the microstructure in 2C_xN⁺2C_l (Br/OAc) were obtained using the cryo-TEM technique. Cryofixation of colloidal dispersions with the controlled environment vitrification system allows microstructural detail of surfactant aggregates as small as 4nm to be clearly seen. Thus bilayers as well as micelles can be visualized with this technique.⁹ Details are given elsewhere.^{8,10,11}

Time-Resolved Fluorescence Quenching (TRFQ)

The use of TRFQ to measure micelle aggregation numbers is well established.^{12,13} A new extension of this technique, described in previous papers^{6,14}, allows dispersions with mixtures of micelles and large aggregates (e.g. vesicles and liposomes) to be studied.

In micelles, the quenching of pyrene fluorescence by DBA following an instantaneous pulse of excitation can be described by the following expression:¹³

$$I(t) = I(0) \exp(-A_2 t - A_3 (1 - \exp(-A_4 t)))$$

where A₂ and A₄ are independent of quencher (DBA) concentration

(for the micellar systems studied here^{6,14}) and represent the rate constant for unquenched fluorescence and the quenching rate constant, respectively. A_3 represents the average number of quenchers per micelle and is given by:

$$A_3 = i[DBA]/[S]_m = \bar{n}i$$

where i is the aggregation number, $[DBA]$ is the quencher concentration, $[S]_m$ is the concentration of surfactant in micellar form (often taken to be the difference between the total surfactant concentration and the critical micelle concentration of the surfactant), and \bar{n} is the scaled quencher concentration.

In vesicles and other large aggregates, the time resolved fluorescence quenching behavior is given by:⁶

$$I(t) = I(0) \exp(-k_{app}t - k_{dot}t^{1/2})$$

where k_{app} and k_{dot} are combinations of various rate constants as described in reference 6. This model does not distinguish between multi- and single-walled aggregates.

Quenching data from solutions containing both micelles and vesicles (or other large aggregates) should logically be described by a model composed of some linear combination of the two rate laws given above. The large number of parameters in such a model, however, frustrates any attempt to numerically fit such data. Fortunately, data from mixed micelle-vesicle systems can be forced to fit the micellar model. When this is done, the values obtained for A_4 show a noticeable dependence on quencher concentration (recall that A_4 is independent of quencher concentration for micellar systems).^{6,13} Of course, quenching data from systems containing no (or very few) micelles cannot be fit at all with the micellar model, and must be analyzed using the alternative (vesicle) rate law given above.

When used together, the three techniques described above can give considerable information about the microstructures present in mixed surfactant systems. TRFQ reveals the presence of micelles in clear and turbid dispersions. In systems containing only micelles, the aggregation number of the micelles can be obtained. VEM and cryo-TEM give detailed structural information on the nature of larger aggregates (for example, these techniques can distinguish single-walled vesicles from multi-walled liposomes).

RESULTS

VEM images of dilute dispersions of $2C_{14}N^+2C_1$ bromide/acetate mixtures are given in Figure 1. As the acetate to bromide ratio increases, we see a progression of microstructures of decreasing size, going from large, multilamellar liposomes at 100% Br⁻ to smaller liposomes and vesicles at 80% Br⁻ (20% OAc⁻), unilamellar vesicles and worms at 60% Br⁻ (40% OAc⁻) and finally a few unilamellar vesicles at bromide contents less than 40%. Cryo-TEM images of similar samples (see Figure 2) confirm the multi-walled to single-walled transition with increasing acetate content. Images at high acetate content contain both single-walled vesicles and small spherical micelles. Finally, TRFQ data (see Figure 3) indicate that no micelles are present in samples containing more than about 50% Br⁻ (i.e., quenching data could only fit with reasonable statistics to the vesicle model). With less than 50% Br⁻, however, the proportion of

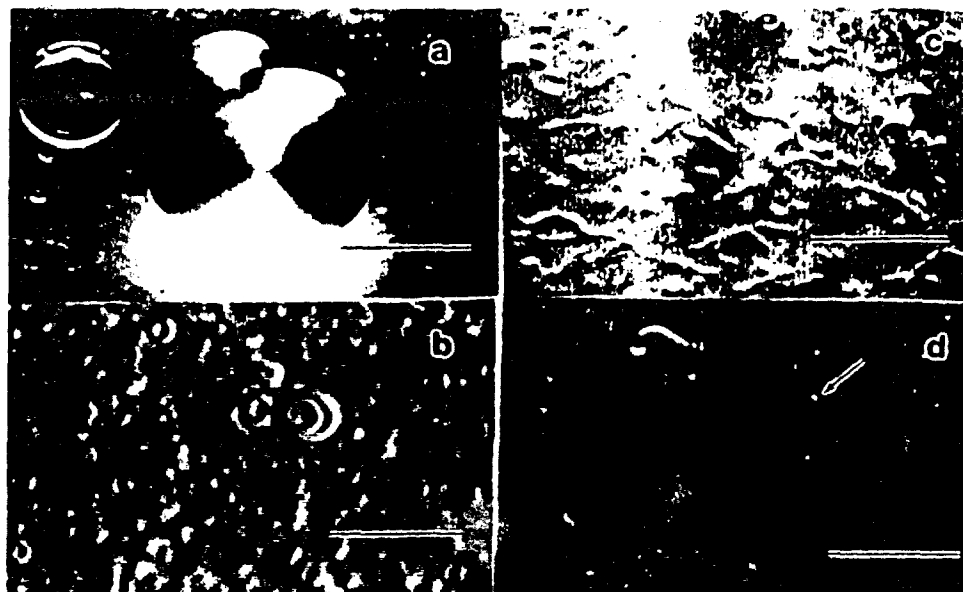


Figure 1. Video enhanced micrographs of 0.002M $2C_{14}N^+2C_1$ aggregates with mixed acetate and bromide counterions. Bar = 10 micron. a) 100% Br^- (0% OAc^-). Large multilamellar liposome with smaller vesicles and liposomes. b) 80% Br^- (20% OAc^-). Large liposomes are absent. The average particle size has decreased. c) 60% Br^- (40% OAc^-). Multilamellar structures have disappeared and are replaced by unilamellar vesicles and worms. Real-time observation on a TV monitor allows vesicles to be seen much more readily due to their Brownian motion. TRFQ indicates that micelles are present in these dispersions as well. d) 40% Br^- (60% OAc^-). Macroscopically clear solution. The number of vesicles (and worms) has decreased. From reference 18.

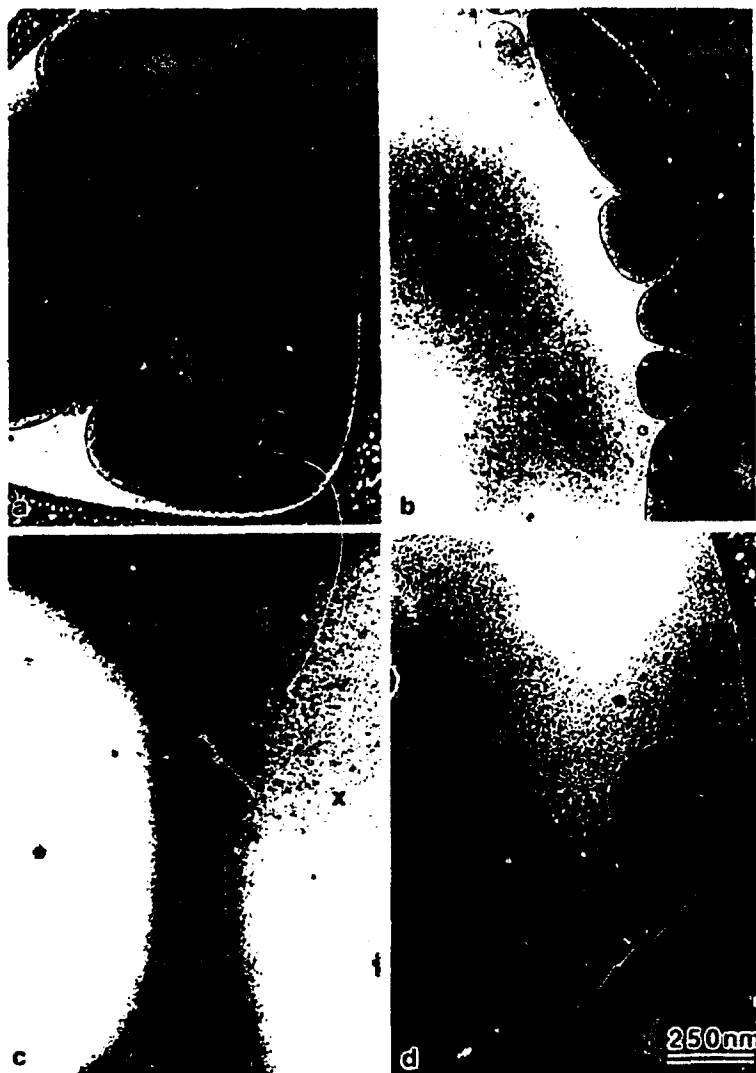


Figure 2. Direct cryo-TEM images of 0.01M $2C_{14}N^{+}2C_{1}^{-}$ dispersions with mixed counterions. a) 100% Br^{-} . Multilayered structures predominate. b) 40% Br^{-} . Unilamellar and bilamellar vesicles predominate. c) 24% Br^{-} . Small ($D = 15$ nm) vesicles coexist with micelles ($D = 6$ nm); the latter are dark spots that are distinct from film grain. d) 0% Br^{-} . Micelles predominate. The bilamellar vesicle seen in this micrograph is most likely the result of residual Br^{-} . From reference 14.

surfactant aggregated in micellar form increases with decreasing bromide content (as evidenced by the decreasing dependence of A_4 on quencher concentration). Below about 26% Br^- , the lack of dependence of A_4 on quencher concentration indicates that very little surfactant is present in vesicles.¹⁴

We note in passing that visual inspection of dispersions of $2\text{C}_{14}\text{N}^+\text{2C}_{14}\text{Br}^-/\text{OAc}^-$ reveals a transformation from milky suspensions at high bromide content to bluish/translucent dispersions at intermediate bromide levels and clear solutions at low bromide content (< ca. 40% Br^-).

Similar behavior is seen in the dicaproylphosphatidylcholine/dipalmitoylphosphatidylcholine ($2\text{C}_{16}\text{PC}/2\text{C}_{16}\text{PC}$) mixture system at 53°C .^{4,14} Dispersions of $2\text{C}_{16}\text{PC}$ are milky white and become progressively less turbid as $2\text{C}_{16}\text{PC}$ is added. Eventually, such dispersions become clear at high $2\text{C}_{16}\text{PC}$ levels. TRFQ results track this progression;¹⁴ pure $2\text{C}_{16}\text{PC}$ dispersions show no evidence of micellar character (i.e. the fluorescence data can only be fit with the vesicle model). As $2\text{C}_{16}\text{PC}$ is added, micelles begin to form. The proportion of micelles grows with increasing $2\text{C}_{16}\text{PC}$ content as seen in the quencher concentration dependence of A_4 (see Figure 4). The NMR data of Gabriel and Roberts⁴ gives strong evidence for unilamellar vesicles in this regime. Finally, with 100% $2\text{C}_{16}\text{PC}$, there is no evidence for any vesicles (hence all aggregates are small micelles). Thus, as in the previous example, we see a transition from liposomes to vesicles to vesicles plus micelles to micelles.

DISCUSSION

How can these results be rationalized? We start by noting that surfactant aggregate size and shape is predicted, at least in dilute solution, by free energy minimization arguments.^{15,16} The free energy of surfactant self-assembly is composed of three parts: 1) a favorable hydrophobic contribution that arises from the burying of the hydrocarbon chains of an amphiphile into the interior of the aggregate, 2) an unfavorable surface term which describes the electrostatic or steric repulsion of the surfactant head groups, and 3) a packing term which considers the size and shape of the amphiphilic molecule and defines accessible geometric shapes for assemblies of these molecules.

Energy minimization results in an optimal aggregate(s) for a given set of conditions. Such aggregates are conveniently described by the surfactant parameter v/al ,¹⁶ where v is the volume of the hydrophobic portion of the molecule, l is the effective length of the hydrocarbon chains and a is the area per surfactant head group. As a first approximation, v is a property of the molecule alone, while l is a function not only of molecular structure but temperature as well. Finally, a reflects molecular structure, temperature and, at least for ionic surfactants, ion binding and ionic strength. Systems in which $v/al < 1/3$ generally form spherical aggregates. The range $1/3 < v/al < 1/2$ defines cylindrical micelles, while $1/2 < v/al < 1$ is the regime of bilayers, vesicles and other large aggregates. Finally, $v/al > 1$ gives inverted structures (such as reversed micelles). Thus, the surfactant parameter is a measure of local curvature.

Because of the large volume per aggregate of double-chained surfactants, such amphiphiles tend to form bilayers, vesicles and other large aggregates; micelles composed of double-chained surfactants are

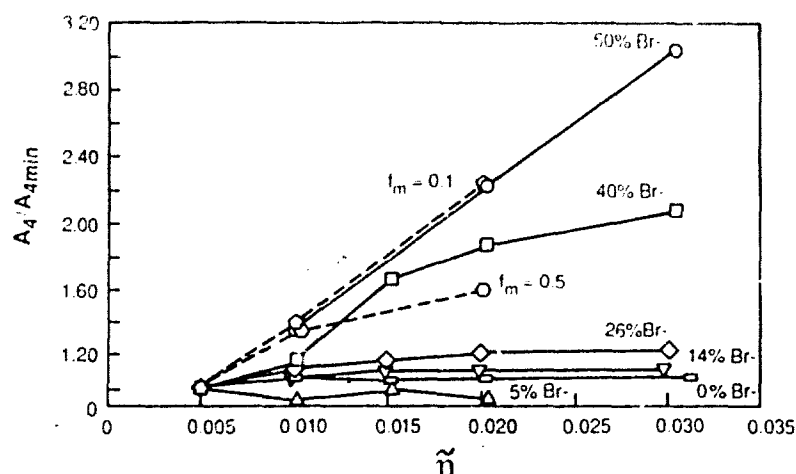


Figure 3. Plot of A_4 vs scaled quencher concentration (\tilde{n}) for $2C_{14}N^+2C_1$ aggregates with mixed bromide and acetate counterions. Values of A_4 have been normalized with respect to A_{4min} (A_4 at $\tilde{n}=0.005$). Also included (dashed lines) are A_4 values obtained from simulations of mixtures of micelles and vesicles (see reference 6). f_m represents the fraction of surfactant in micelle form (i.e. $f_m = 0.1$ represents a simulated dispersion composed of 90% vesicles and 10% micelles). Note that the proportion of surfactant in micelles increases with decreased bromide content.

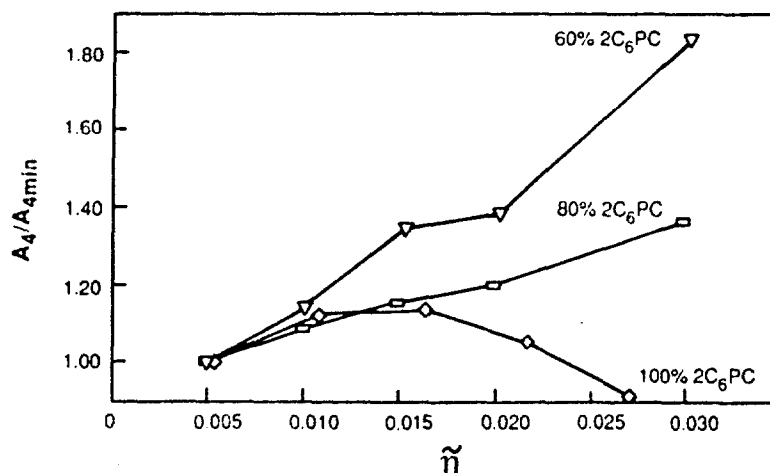


Figure 4. Plot of A_4 vs \tilde{n} for mixtures of $2C_6PC$ and $2C_{16}PC$ at $53^\circ C$. The decreased dependence of A_4 on \tilde{n} with increased $2C_6PC$ content is diagnostic of a vesicle to micelle transition. See text.

generally not observed. Only with short chains or high head group repulsions can double-chained surfactants form micellar aggregates.

To obtain stable, unilamellar vesicles, we require the surfactant parameter to lie between $1/2$ and 1 . However, many other aggregate forms, differing in energy by at most a few kT, are also possible in this curvature regime. In fact, cryo-TEM and VEM studies of several double-chained surfactant systems have revealed the coexistence of liquid crystalline liposomes, vesicles, coiled microtubules and multilayered tubules.^{8,14,17,18} Stabilization of unilamellar vesicles as the dominant aggregate evidently requires bilayer asymmetry in addition to proper curvature control ($1/2 < v/a_l < 1$).^{1,2} Such asymmetry is obtained by employing surfactant mixtures.

Thus, in the dialkyldimethylammonium system, the small, unhydrated bromide counterion sits close to the aggregate surface and shields the electrostatic repulsion between the cationic head groups. As a result, a is small and curvatures are large; dispersions of the bromide surfactant contain many large, liposomal aggregates. The acetate counterion, on the other hand, is highly hydrated and is excluded from the aggregate surface; head group repulsions are high, a is large and curvatures are small. Thus, the optimal aggregate of ditetradecyldimethylammonium acetate is a small, spherical aggregate of aggregation number 60.¹⁴ Mixtures of bromide and acetate counterions give a variety of aggregates as the curvature is tuned. With 40-60% Br⁻, small unilamellar vesicles (in equilibrium with a few micelles) dominate. It is tempting to speculate that such vesicles would possess an asymmetric distribution of counterions; the low (reversed) curvature inner leaf should have more bound bromide than the higher, normally curved inner leaf. Finally, a further decrease in the overall bromide content induces additional curvature and results in an increase in the micelle population and a decrease in the vesicle population.

Similarly, dipalmitoylphosphatidylcholine (2C₁₆PC) forms large liposomes of low curvature, while dicaproylphosphatidylcholine (2C₆PC) forms micelles.⁴ Mixtures of the two give stable vesicles (at 80% 2C₁₆PC), with 2C₆PC occupying, for the most part, only the more highly curved outer leaf of the vesicle bilayer.⁴ As more curvature inducing 2C₆PC is added, micelles grow in number at the expense of vesicles.

CONCLUSIONS

We have seen how mixtures of two surfactants of different inherent curvatures form a progression of structures. Large liposomal aggregates of one surfactant are gradually transformed into micellar aggregates by addition of a second, curvature inducing surfactant. At some intermediate composition, unilamellar vesicles, stabilized by bilayer asymmetry, are formed. As the curvature is further increased, micelles gradually replace vesicles as the dominant aggregate.

The above concept gives a coherent strategy for future research into vesicle stabilization. Such research will have important implications for practical, protein reconstitution work, as well as more fundamental biochemical understanding of cell membrane structure and function.

ACKNOWLEDGEMENTS

This work was supported in part by a grant from the U.S. Army.

also thank J. R. Bellare, E. W. Kaler and S. A. Safran for valuable discussions and insight.

REFERNECES

1. S. Carnie, J. N. Israelachvili, and B. A. Pailthorpe, *Biochimica Biophysica Acta*, **554**, 340 (1979).
2. S. A. Safran, P. Pincus, and D. Andelman, *Science*, **248**, 354 (1990).
3. E. W. Kaler, A. K. Murthy, B. E. Rodriguez, and J. A. N. Zasadzinski, *Science*, **245**, 1371 (1989).
4. N. E. Gabriel and M. F. Roberts, *Biochemistry*, **23**, 4011 (1984).
5. J. E. Brady, D. F. Evans, G. G. Warr, F. Grieser, and B. W. Ninham, *J. Phys. Chem.*, **90**, 1853 (1986).
6. D. D. Miller and D. F. Evans, *J. Phys. Chem.*, **93**, 323 (1989).
7. S. Inoué, "Video Microscopy," Plenum Press, New York, 1986.
8. D. D. Miller, J. R. Bellare, D. F. Evans, Y. Talmon, and B. W. Ninham, *J. Phys. Chem.*, **91**, 674 (1987).
9. J. R. Bellare, T. Kaneko, and D. F. Evans, *Langmuir*, **4**, 1066 (1988); J. L. Burns and Y. Talmon, in "Proceedings of the 45th Annual Meeting of the Electron Microscopy Society of America," G. W. Bailey, Editor, p. 500, San Francisco Press, San Francisco, 1987.
10. M. Adrian, J. Dubochet, J. Lepault, and A. W. McDowell, *Nature*, **308**, 32 (1984).
11. Y. Talmon, *Colloids Surfaces*, **19**, 237 (1986).
12. M. Tachiya, *Chem. Phys. Lett.*, **33**, 289 (1975).
13. M. Almgren and J. E. Löfroth, *J. Colloid Interface Sci.*, **81**, 486 (1981); E. Roelants, E. Geladé, M. Van der Auweraer, Y. Croonen, and F. C. DeSchryver, *J. Colloid Interface Sci.*, **96**, 288 (1983).
14. D. D. Miller, L. J. Magid, and D. F. Evans, *J. Phys. Chem.*, **94**, 5921 (1990).
15. C. Tanford, "The Hydrophobic Effect," 2nd Edition, John Wiley & Sons, New York, 1980.
16. D. J. Mitchell and B. W. Ninham, *J. Chem. Soc. Faraday Trans. 2*, **77**, 601 (1981).
17. D. D. Miller, D. F. Evans, G. G. Warr, J. R. Bellare, and B. W. Ninham, *J. Colloid Interface Sci.*, **116**, 598 (1987).
18. D. D. Miller, J. R. Bellare, T. Kaneko, and D. F. Evans, *Langmuir*, **4**, 1363 (1988).

Accession For	
NTIS GRA&I	<input checked="" type="checkbox"/>
DTIC TAB	<input type="checkbox"/>
Unannounced	<input type="checkbox"/>
Justification	
By	
Distribution/	
Availability Codes	
Dist	Avail and/or Special
A-1	20